



**HAL**  
open science

# Impact of wetting and drying cycles on the mechanical behaviour of a cement-treated soil

Alice Wassermann, Adel Abdallah, Olivier Cuisinier

► **To cite this version:**

Alice Wassermann, Adel Abdallah, Olivier Cuisinier. Impact of wetting and drying cycles on the mechanical behaviour of a cement-treated soil. *Transportation Geotechnics*, inPress, 36, pp.100804. 10.1016/j.trgeo.2022.100804 . hal-03727312

**HAL Id: hal-03727312**

**<https://hal.science/hal-03727312>**

Submitted on 19 Jul 2022

**HAL** is a multi-disciplinary open access archive for the deposit and dissemination of scientific research documents, whether they are published or not. The documents may come from teaching and research institutions in France or abroad, or from public or private research centers.

L'archive ouverte pluridisciplinaire **HAL**, est destinée au dépôt et à la diffusion de documents scientifiques de niveau recherche, publiés ou non, émanant des établissements d'enseignement et de recherche français ou étrangers, des laboratoires publics ou privés.

# 1 Impact of wetting and drying cycles on the mechanical 2 behaviour of a cement-treated soil

3 Alice Wassermann<sup>1</sup>, Adel Abdallah<sup>1</sup>, Olivier Cuisinier<sup>1</sup>

4 <sup>1</sup>LEMETA – Université de Lorraine – CNRS – 54000 Nancy, France

5 Corresponding author:

6 *Alice Wassermann*

7 *Université de Lorraine, CNRS, LEMETA, F-54000 Nancy, France*

8 *2 Rue du Doyen Marcel Roubault - BP 10162*

9 *F-54505 VANDOEUVRE LES NANCY CEDEX*

10 *France*

11 *Email : [alice.wassermann@univ-lorraine.fr](mailto:alice.wassermann@univ-lorraine.fr)*

## 12 **Abstract**

13 The core objective of this study is to analyse the impact of the wetting/drying protocol  
14 on the mechanical behaviour of a cement-treated sand. The impact of two types of  
15 wetting and drying cycles of different magnitudes was evaluated with a quantitative  
16 approach based on the stress-dilatancy approach. The main effect of the  
17 wetting/drying cycles is to alter the bonds and consequently diminish the mechanical  
18 performance. The weathering effect is shown to be dependent on the cement dosage  
19 but also on the intensity of the cycles. For the samples treated with 4% cement, the  
20 very first cycles seem to bring the most alteration of the mechanical performance. For  
21 those treated with 1% cement, however, the accumulation of multiple cycles leads to  
22 more progressive degradation. The evaluation of the bonding ratio permitted the  
23 quantitative assessment of the treatment effect and the weathering progress with  
24 cycles. The results highlight the role of the imposed wetting/drying cycle technique for  
25 a better assessment of the long-term performance of treated soils, even if the definition  
26 of an adequate weathering protocol that makes sense with regard to the real solicitation  
27 endured by engineered structures deserves additional investigation.

28 **Keywords:** Soil stabilization; Triaxial tests; Degradation; Wetting/drying cycles;  
29 Bonding ratio

## 30 **1. INTRODUCTION**

31 Soil treatment with hydraulic binders has been shown to generally improve soil  
32 characteristics such as workability, uniaxial compressive strength (*UCS*) (e.g., [1, 2,  
33 3]), and shear strength (e.g., [4, 5, 6]). Transportations earthen infrastructures built  
34 with stabilized soils such as embankments, pavement subgrades or backfills generally  
35 have an expected lifespan ranging from 50 to 100 years. They should be designed to  
36 undergo cyclic weathering solicitations such as temperature and/or moisture content  
37 variations, in addition to their hydromechanical design loads. Some in situ  
38 investigations of lime-stabilized pavement foundations qualitatively showed that  
39 exposing such structures to varying climatic conditions could have a negative impact  
40 on their mechanical performance in the long term [7, 8, 9]. This was also indicated by  
41 laboratory testing by exposing stabilized soil samples to wetting/drying cycles [10, 11,  
42 12, 13, 14, 15] or freezing/thawing periods [16, 17, 18]. Durability of treated soils is a  
43 subject more and more studied recently [19, 20, 21] as it is now clear that it is essential  
44 to consider the durability of the performance of treated soils in the design process of  
45 such structures, and it is of primary interest to understand the impact of climatic  
46 conditions on the long-term behaviour of stabilized soils.

47 Thus, the development of a methodology for understanding and quantifying the  
48 macroscopic mechanical behaviour degradation of treated soils when exposed to  
49 wetting and drying cycles is necessary. Some authors have assessed the impact of  
50 wetting/drying cycles on the hydromechanical behaviour of stabilized soils. For  
51 instance, Hoy et al. [22] and Cuisinier and Masrouri [23] highlighted that the impact of  
52 hydric cycles on the *UCS* was dependent on the type of binder used. Cuisinier and  
53 Masrouri [23] found that after 90 days, the *USC* was approximately two times higher  
54 with 3% CEM II than with 3% lime. After 6 cycles, the *UCS* was still 100 kPa higher  
55 with cement than with lime. Rao et al. [10] showed that this impact was also a function  
56 of the dosage of binders, which was confirmed by several authors [24, 25]. Some  
57 authors [10, 26, 27] have shown that the extent of degradation is related to the  
58 mineralogical composition of the tested soil. Another very important aspect is the  
59 experimental protocol employed to perform the cycles in the laboratory. Indeed,  
60 several methods for imposing drying/wetting cycles have been used by different  
61 authors with varying durations for the wetting and drying phases, the method used for  
62 wetting (capillary rise or immersion), and the temperature during the drying phase (air-

63 drying or oven-drying). The majority of past studies employed methods derived from  
64 the ASTM D559 standard [28], which recommends 5 hours of immersion in water at  
65 room temperature, followed by 42 hours in an oven at 71 °C. For instance, Chittoori et  
66 al. [13] worked on 7-day cured lime-treated clayey soils (6 and 8% lime) and performed  
67 *UCS* tests after 3, 7, 14 and 21 cycles following the ASTM D 559 method. They  
68 observed considerable strength loss with an increasing number of cycles. For example,  
69 on samples treated with 6% lime, they reported a *UCS* decrease of 15% after 3 cycles  
70 and a complete loss of strength after 12 cycles. Consoli et al. [25] studied the  
71 accumulated mass loss and *UCS* evolution after a 12-cycle recurrent wetting/drying  
72 series followed by brushing strokes on a fine-grained soil treated with cement (CEM I  
73 type). ASTM D559 cycles were then performed. The authors observed that the *UCS*  
74 first increased after 3 cycles and then decreased (for 3% and 6% cement) or tended  
75 to fluctuate around an average (for 9% cement). They attributed these results to the  
76 possible acceleration of the cementitious reactions due to increasing temperature  
77 during the drying portion of the very first cycles. The original ASTM cycles could,  
78 however, be considered relatively severe compared to the conditions to which treated  
79 soil could be exposed in situ. Some other authors who have used suction control  
80 techniques for wetting/drying cycles reported that the higher the magnitude of the  
81 wetting/drying cycles is, the higher the performance degradation ratio [9, 24, 29, 30].  
82 Therefore, employing an aggressive method may lead to overly conservative  
83 conclusions about the long-term performance of a given stabilized soil exposed to  
84 wetting/drying cycles. The impact of the different types of weathering cycles still needs  
85 to be investigated.

86 Beyond the experimental protocols for wetting/drying cycles, a key aspect is the  
87 quantification of the effects of these cycles. Most of the studies available in the  
88 literature based their analysis on the monitoring of the mass loss of the samples and/or  
89 the *UCS* as a function of the number of cycles applied [31, 32, 27, 25, 23]. However,  
90 these macroscopic indicators do not permit a full understanding of the degradation  
91 process of the mechanical behaviour associated with the cycles. The evolution of the  
92 interparticle bonding associated with the treatment after weathering cycles is of primary  
93 interest for evaluating and discussing the degradation mechanism and to provide  
94 further understanding of the treated soil behaviour. Two main approaches can be found  
95 in the literature to this end. The first one is based on an explicit quantification of the

96 cementitious products as a function of the treatment conditions. This quantification can  
97 be performed through chemical or microstructural analyses. In a few studies, the  
98 relationship between mechanical characteristics and the amount of cementitious  
99 products was investigated (e.g., [33, 34]). For instance, Dadda et al. [35] investigated  
100 the biocementation process effect on the micromechanical properties (coordination  
101 number, contact surface, and volume fraction of calcite) of biocemented Fontainebleau  
102 sand. This study managed to link the cohesion of the biocemented sand to the  
103 evolution of the cohesive surface and other micromechanical properties within the sand  
104 specimen using high resolution 3D images obtained by X-ray synchrotron  
105 microtomography. This study led to the development of a linear equation relating the  
106 cohesion, mean coordination number and contact surface formed by the cementation  
107 agent. However, these methods work with many uncertainties, and it is difficult to  
108 explicitly establish the link between the quantity of cementitious products and the  
109 macroscopic behaviour. In the second approach, the effects of cementation are  
110 quantified indirectly through the analysis of the mechanical behaviour. In this case, the  
111 behaviour of the untreated soil is usually taken as a reference (e.g., [36, 37, 38]). For  
112 example, the results from triaxial tests were interpreted using the stress-dilatancy  
113 theory [39, 40] by Wang et al. [41] to compare the mechanical behaviour between  
114 biocemented and cement-treated sand. This approach allowed the bond breakage, the  
115 development of dilatancy and the bonding mobilization to be analysed. These methods  
116 could lead to a sharper analysis of the mechanical behaviour of treated soils by  
117 highlighting the impact of the treatments.

118 The literature review shows that the quantitative impact of the wetting/drying cycling  
119 protocol is still an open-ended question, as is the analysis of the degradation process.  
120 In this context, the first objective of this study is to analyse the impact of the  
121 wetting/drying protocol on the mechanical behaviour of a cement-treated sand. Two  
122 types of weathering cycles of different magnitudes will be compared. The second  
123 objective is to develop a quantitative analysis of performance degradation with the  
124 number of cycles. The mechanical analysis is based on a stress-dilatancy approach  
125 using triaxial compression tests.

126 First, the materials and methods will be detailed, including a theoretical background on  
127 the stress-dilatancy approach on which the results analysis is based. Then, the  
128 experimental program will be exposed. The analysis of the treatment effects and the

129 impact of the wetting/drying cycles on the mechanical behaviour and on the bonding  
130 ratio will be successively presented. This will be followed by a discussion and a  
131 conclusion.

## 132 **2. MATERIALS AND METHODS**

### 133 **2.1. Tested materials**

134 The selected soil is a sand sampled in the eastern part of France. It has been classified  
135 as an S1-type soil according to the French classification system [42] and an SW soil  
136 according to the Unified Soil Classification System (Table 1 and Fig. 1) [43]. On Fig. 1,  
137 the red lines represent the  $D_{10}$ ,  $D_{30}$  and  $D_{60}$  (from bottom to top of the graph) that are  
138 used to determine the measures of gradation. From the grain-size distribution it is possible  
139 to calculate uniformity coefficient,  $C_u$ , and the coefficient of curvature,  $C_c$ , respectively  
140 5.88 and 1.24. The soil is considered as well-graded. The absorption coefficient of the  
141 sand is 1.50%.

142 The selected cement in this study is Portland cement (CEM I 52,5 N) containing at  
143 least 95% clinker. The specific gravity considered for this type of cement is 3.15.  
144 Compressive strength tests on this cement showed that 97% of the maximum strength  
145 was reached after 7 days, as per the NF EN 196-1 standard [44]. A cement setting test  
146 was also performed, and the measured setting time was 2 h 50 min [45].

### 147 **2.2. Specimen preparation**

148 All of the samples were prepared at a target dry density of  $1.7 \text{ Mg.m}^{-3}$ , corresponding  
149 to a relative density of 84%. The preparation water content was set to 7% to ensure  
150 complete hydration of the cement. The preparation of the samples started by mixing  
151 the dry sand with the cement. Then, water was added while mixing continued for five  
152 minutes until the mixture became homogeneous. The samples were prepared in  
153 cylindrical two-part moulds to facilitate unmoulding. Each sample was compacted by  
154 axial compression according to the standard for the treated soils [46] in three layers to  
155 minimize the density gradient along the vertical axis. The specimen have a diameter  
156 of 50 mm and a height of 100 mm. After compaction, the samples were wrapped up in  
157 a plastic sheet to prevent any exchange with the environment. They were then stored  
158 in a controlled temperature room at  $20 \text{ }^\circ\text{C}$  for 14 days. This curing time was chosen  
159 after preliminary compression tests that showed that *UCS* tends to be stabilized after  
160 14 days.

161 **2.3. Triaxial tests**

162 A conventional triaxial system apparatus was used to carry out consolidated drained  
163 (CD) tests. The samples were considered to be saturated once Skempton's B-value  
164 was higher than 0.95. Three confining effective pressures were applied: 50 kPa, 100  
165 kPa and 200 kPa. The shearing velocity was fixed at 0.1mm/min. This shearing velocity  
166 was selected to ensure fully drained conditions during the test. The pressure was  
167 applied with advanced pressure volume controllers with a precision of 2 kPa, and the  
168 volume measurements were made with an accuracy of 0.1 cm<sup>3</sup>.

169 **2.4. Wetting and drying cycle protocols**

170 Two different methods of wetting/drying cycles were employed to study the impact of  
171 the intensity of the cycles on the mechanical behaviour: type I with high intensity and  
172 type II with moderate intensity. The type I cycle was derived from the ASTM standard  
173 D559 [28]. The wetting process consisted of immersing the samples in water at room  
174 temperature for 8 hours. The samples were then oven-dried for 16 hours at 65 °C. The  
175 type II cycle was inspired by the literature [12, 47]. The wetting process was performed  
176 by immersion in water for 48 hours. Complete samples immersion has been selected  
177 as the worst case wetting condition. It leads to a fast total saturation of the material  
178 and permits leaching of cementitious compounds. The drying phase was conducted in  
179 a climatic chamber (SECASI Technologies SH-600 ©) at a temperature of 20 °C and  
180 a relative humidity of 50% for 120 hours. The water content variations in the samples  
181 were monitored to ensure that 5 days was suitable to dry the samples (for the ten first  
182 type I cycles, the water content variations after a wetting and a drying phase ranged  
183 from 21.6% to 23.7%). For instance, photos of samples 4% cement treated samples  
184 after 3 and 6 cycles are presented in Fig. 2. After 6 type-I cycles, the 4%-cement-  
185 treated samples still visually seem intact. These drying conditions were selected to  
186 correspond to the weather conditions that are generally experienced during the  
187 summer in the northern part of France. The type II cycle is regarded as less  
188 "aggressive" than the type I cycle. It is intended to impose weathering in compliance  
189 with the environmental conditions to which an engineered structure is expected to be  
190 submitted during its lifespan.

191 **2.5. Quantification of the bonding effect**

192 The chosen approach for the quantification of the bonding effect is based on Rowe's  
193 stress-dilatancy theoretical framework for frictional cohesive materials [39]. The

194 dilatancy ratio  $d$  is defined as the ratio of the increment of the plastic volumetric strains  
 195  $\delta\varepsilon_v^p$  and the increment of plastic shear strains  $\delta\varepsilon_s^p$ .

$$d = -\frac{\delta\varepsilon_v^p}{\delta\varepsilon_s^p} \quad (1)$$

196 This ratio can be calculated via the following total strain increments:

$$\delta\varepsilon_v = \delta\varepsilon_1 + 2\delta\varepsilon_3 \quad (2)$$

$$\delta\varepsilon_s = \frac{2}{3}(\delta\varepsilon_1 - \delta\varepsilon_3) \quad (3)$$

197 where  $\delta\varepsilon_1$  and  $\delta\varepsilon_3$  are the strain increments in the directions of the major and minor  
 198 principal stresses, respectively.

199 Cuccovillo and Coop [40] used the stress-dilatancy theory formulated in terms of  
 200 energy for the analysis of the failure of cementitious bonds. They suggested that the  
 201 total work of a cemented soil sample subjected to shear  $\Delta W$  corresponds to the loss  
 202 due to friction on the one hand ( $\Delta W_{fric}$ ) and to the failure of the cementitious bonds  
 203 on the other hand ( $\Delta W_{bond}$ ).

$$\Delta W = \Delta W_{fric} + \Delta W_{bond} \quad (4)$$

204 Under axisymmetric conditions, the total work can be written as follows:

$$\Delta W = q \delta\varepsilon_s^p + p' \delta\varepsilon_v^p \quad (5)$$

205 where  $q$  is the deviator stress and  $p'$  is the mean effective stress.

206 In the framework of the original Cam-Clay model,  $\Delta W_{fric}$  was defined by Roscoe et al.  
 207 [48] as:

$$\Delta W_{fric} = Mp' \delta\varepsilon_s^p \quad (6)$$

208 where  $M$  is the slope of the critical state line. Combining Equations (4), (5) and (6)  
 209 leads to:

$$q\delta\varepsilon_s^p + p'\delta\varepsilon_v^p = Mp' \delta\varepsilon_s^p + \Delta W_{bond} \quad \text{so} \quad \frac{q}{p'} = M - \frac{\delta\varepsilon_v^p}{\delta\varepsilon_s^p} + \frac{\Delta W_{bond}}{p'\delta\varepsilon_s^p} \quad (7)$$

210  $\frac{q}{p'} = \eta$  is defined as the ratio of deviator and mean stresses.

211 Equation (7) shows that the stress ratio  $\eta$  at the critical state is a function of  $M$ ,  $d$  and  
 212 the work dissipated due to the destruction of the cementitious bonds. One can derive  
 213 the bonding effect due to the cement action by:

$$\eta_{bond} = \frac{\Delta W_{bond}}{p' \delta \varepsilon_s^p} \quad (8)$$

214 This ratio is equal to 0 for untreated sand because there is no bonding effect. Finally,  
 215 the following equation can be written:

$$\eta = M + d + \eta_{bond} \quad \text{so} \quad \eta - d = M + \eta_{bond} \quad (9)$$

216 Wang et al. [41] proposed a comparison between the cementation of a sand induced  
 217 by biological action and the cementation induced by the addition of a cement trough  
 218 by studying the dilatancy behaviour of the material during drained triaxial tests. This  
 219 approach provides a methodology for the monitoring of the shearing behaviour by  
 220 scanning the evolution of 5 points, as represented in Fig. 3. Point A represents the  
 221 inflection point of the tangent modulus evolution during shearing. It can be defined as  
 222 a yielding point according to the definition of Malandraki and Toll [49] as a transition  
 223 from a constant stiffness to a stiffness degradation response. Physically, it corresponds  
 224 to the initiation of the breaking of cementitious bonds for a treated soil. Point B is the  
 225 maximum of the deviator stress. The material switches at this point from contracting to  
 226 dilative behaviour. Point C is the maximum dilatancy ratio. After the yield point (point  
 227 A), an increasing number of bonds break out causing the material to expand until point  
 228 C. Before this point, the dilation is hindered by the mobilization of the strength of the  
 229 cementitious bonds. Point D represents the stage where the deviator stress and the  
 230 dilatancy become constant and is determined preferentially on the volumetric-strain  
 231 curve. This point represents the beginning of the residual state of the soil behaviour  
 232 and zero dilatancy (the critical state). Point X is the maximum bonding ratio indicating  
 233 the strength of the cementitious bonds. The evolution of the bonding ratio during a  
 234 triaxial test is illustrated in Fig. 4 for a specimen treated with 6% cement under a  
 235 confining pressure of 50 kPa. For untreated soils, an additional point of interest is point  
 236 E, located at the end of the test because there are no cementitious bonds. It is worth  
 237 noting that even if the interpretation of the bonding ratio might not be relevant after the  
 238 peak, due to the failure localization, it could provide interesting insight into the  
 239 remaining unbroken bonds. In this study, reference points A, B, C, D and X will be  
 240 monitored, and the bonding ratio will be assessed to determine the potential  
 241 degradation after the wetting/drying cycles.

## 242 **2.6. Test repeatability**

243 In this study, the radial strains were not measured directly but calculated from the  
244 volume strain and axial strain based on the right cylinder assumption. The right cylinder  
245 assumption is commonly adopted for correcting the sample section during drained  
246 shearing using axial and volumetric deformations [50]. The values of volumetric strain  
247 may be subject to small errors due to membrane effects but also because of the  
248 degradation of the samples. This strategy was used to limit the potential deleterious  
249 impact of internal sensor installation on the sample exposed to several wetting/drying  
250 cycles and the associated mechanical degradation. Therefore, a careful experimental  
251 protocol was established to ensure the repeatability of the measurements.

252 In this context, several repeatability tests were performed, especially to check the  
253 estimation of the bonding ratio. As an example, two specimens treated with 6% cement  
254 were made and cured for 14 days. Then, triaxial tests were performed (Fig. 5). The  
255 maximum deviator stress varied from 1913 to 1983 kPa, and the peak was located  
256 between 0.9 and 1.2% of the axial strain. The residual deviator stress ranged from 80  
257 to 100 kPa. The  $E_{50}$  modulus ranged from 2.1 to 2.3 MPa. The impact of the preparation  
258 and the execution of the triaxial tests on the bonding ratio was also assessed (Fig. 5).  
259 Between the three specimens, the maximum bonding ratio ranged from 2.013 to 2.313.  
260 This peak is observed between 0.3 and 0.5% axial strain. The bonding ratio also tends  
261 toward 0 at approximately the same axial strain (1.7%). The post peak behaviour  
262 appeared to be significantly different, which was attributed to the localization of the  
263 deformation during the test and was not considered and analysed in terms of the  
264 bonding ratio.

265 Therefore, these tests confirmed that the experimental protocol allowed us to  
266 conveniently determine the bonding ratio from the start of the test up to the peak shear  
267 strength.

## 268 **3. EXPERIMENTAL PROGRAM**

269 The experimental program was divided into two parts. The first aim is to investigate the  
270 influence of the cement content and confining pressure on the mechanical behaviour.  
271 To this end, a range between 1% and 6% was considered for the cement content, and  
272 three confining pressure values were selected: 50, 100 and 200 kPa. The second part  
273 investigates the impact of weathering on the mechanical properties. To this end,

274 specimens prepared with 1% and 4% cement contents were submitted to  
275 wetting/drying cycles. The triaxial tests were only performed under an intermediate  
276 confining pressure of 100 kPa. Each specimen was duplicated with a control specimen  
277 that was prepared at the same time and stored under controlled room temperature in  
278 sealed conditions. The control specimen was not subjected to any hydric cycles, while  
279 the test sample was subjected to wetting/drying cycles. The triaxial tests were then  
280 performed the same day on the two samples. This procedure is intended to assess the  
281 degradation of the mechanical behaviour after the cycles.

## 282 **4. ANALYSIS OF TREATMENT EFFECTS**

283 In this section, the different results and interpretations obtained from experiments are  
284 presented in two different parts, first the analysis of the treatment effects and then the  
285 impact of the wetting and drying cycles.

### 286 **4.1. Stress–strain behaviour**

287 Fig. 6 and Fig. 7 show the stress–strain and volumetric-strain curves for the three  
288 confining pressures studied, respectively. The untreated sand is taken as a reference  
289 for comparison purposes. It can be observed from the stress–strain curves that the soil  
290 behaviour evolves from ductile to brittle as the cement dosage increases. The  $E_{50}$   
291 modulus increases sharply as the dosage increases from 1% to 4% and remains  
292 almost constant from 4% to 6%. For the higher dosage, dilatancy appears for smaller  
293 axial strains. The increase in confining pressure delays the appearance of dilatancy  
294 and lowers the residual value of volumetric strain.

295 For the untreated sand, the friction angle is  $37^\circ$ . The corresponding  $M$  for the studied  
296 sand is evaluated to be 1.24. The cohesion and friction angle for each cement content  
297 are given in Table 2. The cohesion increases by 8 times between 1 and 6%, while the  
298 friction angle increases slightly, which is in accordance with the reported trends in the  
299 literature [51, 52].

### 300 **4.2. Bonding ratio**

301 For a 1% cement ratio, the maximum bonding ratio is equal to 0.337 under a 100 kPa  
302 confining pressure. This value triples with 2% cement and is multiplied by 6 with 6%  
303 cement, as shown in Fig. 8. The maximum bonding ratio is positively correlated with  
304 the cement content. The increase in the confining pressure tends to decrease the  
305 maximum bonding ratio, indicating that bond breaking during the application could

306 have occurred under isotropic pressure. The peak value of the bonding ratio can be  
307 decreased up to 50%, for example, for 4% cement from a confining pressure of 50 kPa  
308 to 200 kPa. The higher the cement content is, the less sensitive the sample appears  
309 to be to the increase in confining pressure.

310 The values of points A, B, C, D and X determined for all of the tests are presented in  
311 Table 3. Point A globally shifts towards smaller axial strains with increasing cement  
312 content, which indicates that the cementitious bonds start breaking at lower axial  
313 deformation. This also reflects that the  $E_{50}$  modulus increases between cement  
314 contents of 1% and 6%. Concerning the maximum dilatancy (point C), the higher the  
315 cement content is, the higher the deviator stress and the lower the axial strain,  
316 indicating that the material becomes more dilative.

### 317 **4.3. Impact of the wetting/drying cycles**

318 In this study, the mass loss of the samples was monitored through all the cycles. For  
319 the samples treated with 1% after 9 type-I cycles the mass loss is -7,6% and -6,8%  
320 after 9 cycles type II. For the samples treated with 4% the mass loss is -4,8% after 9  
321 type-I cycles as well as type-II cycles. Fig. 9 and Fig. 10 highlight the impact of the  
322 cycle types on the mechanical behaviour for each dosage. Table 4 and Table 5 provide  
323 a more detailed analysis of the graphs according to the Wang et al. [41] method with  
324 points A, B, C, D and X. For each dosage, the control specimen was taken as a  
325 reference to evaluate the degradation of the mechanical parameters. Although an  
326 alteration of the mechanical performance can be observed, after nine cycles, the  
327 samples are not totally destroyed, and triaxial tests can still be performed at both  
328 dosages. Two distinct trends can be observed depending on the cement content.  
329 Concerning the samples treated with 1% cement, the type I cycles show progressive  
330 degradation with the number of cycles (Fig. 9.a). However, it is difficult to observe a  
331 clear pattern with cycle II (Fig. 9.b). The maximum deviator stress is equal to 130 kPa  
332 after 9 high-intensity cycles (type I) and 560 kPa after 9 moderate-intensity cycles (type  
333 II), while the control specimen has a maximum deviator stress of 590 kPa. The type I  
334 cycles do not seem to affect the volumetric behaviour for the material treated with 1%  
335 cement. After type II cycles, however, dilation is delayed and tends to increase. Indeed,  
336 the dilatancy decreases steadily with the number of high-intensity cycles. It can be  
337 observed that the maximum deviator stress decreases the most between 6 and 9 type  
338 I cycles. These later cycles account for the major part of the degradation. For the type

339 II cycles, the accumulation of cycles has an observable effect on the volumetric  
340 behaviour. Indeed, the volumetric strain becomes positive (dilatative behaviour) for  
341 higher axial strains for a greater number of cycles. For the bonding ratio, the maximum  
342 for the control specimen is 0.6. Cycle I affect the bonding ratio and its maximum for a  
343 sample with 1% cement, as shown in Fig. 11.a. In contrast, the type II cycles do not  
344 seem to truly affect the bonding ratio, and no clear pattern can be identified (Fig. 11.b).  
345 For the deviator stress, the last type I cycles seem to impose a greater alteration of the  
346 bonding ratio.

347 In contrast to the samples treated with 1% cement, for the 4% cement dosage, the first  
348 type I cycle seems to condition the material behaviour of the samples. The control  
349 specimen treated with 4% cement has a maximum deviator,  $q_{max}$ , stress of  
350 approximately 1550 kPa (almost 3 times higher than the control specimen treated with  
351 1% cement). For the samples treated with 4% cement, the maximum deviator stress is  
352 decreased by 430 kPa after 9 type I cycles (Fig. 10.a). For the type II cycles (Fig. 10.b),  
353 the maximum deviator stress is reduced by 170 kPa after 9 cycles (but  $q_{max}$  is  
354 decreased by 290 kPa after only 1 cycle, and the pattern is not clear for these cycles).  
355 The volumetric behaviour is slightly modified for the samples treated with 4% cement  
356 after type I cycles, mostly regarding the dilatant behaviour. This behaviour is not  
357 modified for the type II cycles for a cement content of 4%, as presented in Fig. 10.b.  
358 Indeed, the maximum deviator stress decreases by 26% between the control specimen  
359 and the specimen after one wetting/drying cycle and remains constant after 6 and 9  
360 cycles. Regarding the volumetric behaviour, the accumulation of type I cycles for 4%  
361 cement causes a slight decrease in the dilatancy, which seems to be stabilized after  
362 six cycles. For the bonding ratio, the maximum for the control specimen is  
363 approximately 1.8. The type I cycles lowered the maximum bonding ratio to 1.3 (Fig.  
364 12.a), whereas no clear pattern can be observed for the type II cycles. However, a  
365 greater impact is seen after 1 cycle and decreases the maximum  $\eta_{bond}$  to approximately  
366 1.6 (Fig. 12.b).

## 367 5. DISCUSSION

368 This study highlights the impact of the type and number of hydric cycles as well as the  
369 cement content on the mechanical behaviour. This alteration results in a decrease in  
370 the maximum deviator stress but also the maximum bonding ratio. For further analysis,  
371 we can now examine the dilatancy. It is possible to assess the weathering of the

372 specimens by plotting the stress-dilatancy curves and comparing the control  
373 specimens with the results obtained after 9 cycles of both types. For type I cycles and  
374 in the case of a 1% cement dosage, the maximum dilatancy ratio changes from 1.2 to  
375 0.75, and the yield point is reached for a lower stress ratio. The observations are similar  
376 for the 4% cement dosage to a lesser extent. The maximum dilatancy ratio ranges  
377 between 1.7 and 1.97. For 1% (Fig. 13.a) and 4% (Fig. 13.b) cement-treated  
378 specimens, it can be seen that the type II cycles do not significantly affect the maximum  
379 dilatancy, the maximum deviator stress or the yield point.

380 The bonding ratio is not affected by the type II cycles, as its value remains almost  
381 constant, whereas it decreases with the number of type I cycles (Fig. 14). The type II  
382 cycles are considered less “aggressive” and lead to a very slight alteration for this type  
383 of soil and treatment. As previously seen for the maximum strength, the 9<sup>th</sup> cycle seems  
384 to have a higher impact on the specimens treated with 1% cement, whereas for the  
385 specimens treated with 4%, the effect appears after the first cycle. The contrast  
386 between the bonding ratio after cycles of different intensities increases with the number  
387 of cycles. The analysis of the bonding ratio also revealed that it was more difficult to  
388 interpret the results for 1% than for 4% because of the significant noise observed in  
389 the data.

390 From the obtained results on the two considered cement contents after several cycles,  
391 it can be observed, for instance, that the maximum deviator stress can be higher after  
392 the very first cycles than the value of the control specimen. This observation is made  
393 for the type II cycles. This is in agreement with the observation by Consoli et al. [25],  
394 who observed that the UCS of cement-treated sand tends to increase during the first  
395 cycles. The mass loss and the moisture content were monitored through the whole  
396 cycles and we can also notice this trend. The moisture content is higher during the first  
397 cycles for both dosages and both cycle types. Then, there is no significant differences  
398 of moisture content for the two cycle types. The mass loss is almost similar for the  
399 samples treated with 4% after the two types of cycles. For the samples treated with  
400 1%, there is an additional 1% mass loss after the type-I cycles. The moisture content  
401 is always higher during the first cycles and then it stabilized. For 4%-cement it varies  
402 between 5% (dry phase) and 11% (wet state) for both type of cycles. For 1%, the  
403 variations go from 6% to 15% for type I cycles and 6% to 12% for type II cycles.  
404 Between the two types of cycles, the parameters that varies are the duration of the

405 cycles but mostly the heat of the drying phase. A few studies (e.g., [53, 54]) have  
406 assessed the effect of temperature on several parameters such as wettability of the  
407 samples or modulus of rupture. It has been shown that high temperatures (during  
408 wetting or drying phases) affect the samples and reduce the strength. Exposing the  
409 samples to water and heat is most likely to reactivate the cement hydration reactions  
410 and so the physico-chemical processes, leading to the creation of new bonds and an  
411 increase in the soil strength [24, 55].

## 412 **6. CONCLUSION**

413 This study aimed to assess the impact of the cement content on the mechanical  
414 behaviour of cement-treated sand and to evaluate the impact of the intensity and  
415 number of wetting/drying cycles on the mechanical performance. This evaluation is  
416 based on a stress-dilatancy approach and, in particular, on indirect evaluation of the  
417 bonding ratio, which measures the gain of mechanical performance brought by the  
418 treatment.

419 The following conclusions can be drawn from the study.

- 420 - The material brittleness increases with increasing cement content, and the yield  
421 point is obtained for a smaller axial strain. Moreover, the bonding ratio increases  
422 with the cement dosage and tends to decrease with increasing confining  
423 pressure. There is thus a positive relationship between the bonding ratio and  
424 the amount of binder added to the soil.
- 425 - The main effect of the wetting/drying cycles is to alter the bonds and  
426 consequently diminish the mechanical performance. This alteration is  
427 dependent on the initial cement content but also on the intensity of the cycles.  
428 Indeed, the type I cycles, which are more aggressive, lead to a greater  
429 degradation than the type II cycles. The latter were intended to be more  
430 representative of the expected solicitations to which engineered structures can  
431 be submitted during their lifespan.
- 432 - The weathering effect is shown to be dependent on the cement dosage. For the  
433 samples treated with 4% cement, the very first cycles seem to bring about the  
434 most alteration of the mechanical performance. For those treated with 1%  
435 cement, however, the accumulation of multiple cycles leads to more progressive  
436 degradation. The evaluation of the bonding ratio permitted the quantitative

437 assessment of the treatment effect and the weathering progress with cycles.  
438 Nevertheless, it is worth noting that the accuracy of this ratio is in question when  
439 the cement dosage is low and that its validity after soil yielding might be called  
440 into question.

441 - The results highlight the role of the imposed wetting/drying cycle technique for  
442 a better assessment of the long-term performance of treated soils even if the  
443 definition of an adequate weathering protocol that makes sense with regard to  
444 the real solicitation endured by engineered structures deserves additional  
445 investigation.

446

447 To further confirm the observed trends, samples treated with 1% and 4% will undergo  
448 a larger number of type I and II cycles (12, 15, 18 and up to 21 cycles). The results  
449 suggest that it would be interesting to consider studying the samples at the microscopic  
450 scale, with SEM observations for example, to analyse the distribution of cementitious  
451 bonds and better understand the alteration mechanisms.

## 452 **7. ACKNOWLEDGMENTS**

453 The project has received funding from the European Union's Horizon 2020 research  
454 and innovation programme under the Marie Skłodowska-Curie grant agreement No  
455 778120.

## 456 **8. NOTATION**

457  $d$  = dilatancy ratio

458  $M$  = slope of the critical state line

459  $p'$  = mean effective stress

460  $q$  = deviator stress

461  $UCS$  = uniaxial compression strength

462  $\delta\varepsilon_1$  = strain increments in the direction of the major principal stress

463  $\delta\varepsilon_3$  = strain increments in the direction of the minor principal stress

464  $\delta\varepsilon_v^p$  = increment of the plastic volumetric strains

465  $\delta\varepsilon_s^p$  = increment of the plastic shear strains

466  $\Delta W$  = total work  
467  $\Delta W_{bond}$  = energy loss due to the cementitious bonds' failure  
468  $\Delta W_{fric}$  = energy loss due to friction  
469  $\eta$  = ratio of deviator and mean stresses  
470  $\eta_{bond}$  = bonding ratio

## 471 9. REFERENCES

- 472 [1] Consoli NC, Prietto PDM, da Silva Lopes L, Winter D. Control factors for the long  
473 term compressive strength of lime treated sandy clay soil. *Transportation*  
474 *Geotechnics* 2014;1:129–36. <https://doi.org/10.1016/j.trgeo.2014.07.005>.  
475 [2] Nguyen LC, Inui T, Ikeda K, Katsumi T. Aging effects on the mechanical property  
476 of waste mixture in coastal landfill sites. *Soils and Foundations* 2015;55:1441–53.  
477 <https://doi.org/10.1016/j.sandf.2015.10.009>.  
478 [3] Baldovino JA, Moreira EB, Teixeira W, Izzo RLS, Rose JL. Effects of lime addition  
479 on geotechnical properties of sedimentary soil in Curitiba, Brazil. *Journal of Rock*  
480 *Mechanics and Geotechnical Engineering* 2018;10:188–94.  
481 <https://doi.org/10.1016/j.jrmge.2017.10.001>.  
482 [4] Brandl H. *Alteration of Soil Parameters by Stabilization with Lime*, 1981, p. 587–  
483 94.  
484 [5] Attoh-Okine NO. Lime treatment of laterite soils and gravels — revisited.  
485 *Construction and Building Materials* 1995;9:283–7. [https://doi.org/10.1016/0950-](https://doi.org/10.1016/0950-0618(95)00030-J)  
486 [0618\(95\)00030-J](https://doi.org/10.1016/0950-0618(95)00030-J).  
487 [6] Poncelet N, François B. Effect of laboratory compaction mode, density and  
488 suction on the tensile strength of a lime-treated silty soil. *Transportation*  
489 *Geotechnics* 2022;34:100763. <https://doi.org/10.1016/j.trgeo.2022.100763>.  
490 [7] Gutschick KA. *Lime stabilization under hydraulic conditions.*, 1978, p. 1–20.  
491 [8] Kelley CM. *A long range durability study of lime stabilized bases at military posts*  
492 *in the southwest*. National Lime Association, 1988;Bulletin 328.  
493 [9] Cuisinier O, Deneele D. *Long-term behaviour of lime-treated expansive soil*  
494 *submitted to cyclic wetting and drying*, 2008.  
495 <https://doi.org/10.1201/9780203884430>.  
496 [10] Rao SM, Reddy BVV, Muttharam M. The impact of cyclic wetting and drying on  
497 the swelling behaviour of stabilized expansive soils. *Engineering Geology*  
498 2001;60:223–33. [https://doi.org/10.1016/S0013-7952\(00\)00103-4](https://doi.org/10.1016/S0013-7952(00)00103-4).  
499 [11] Guney Y, Sari D, Cetin M, Tuncan M. Impact of cyclic wetting–drying on swelling  
500 behavior of lime-stabilized soil. *Building and Environment* 2007;42:681–8.  
501 <https://doi.org/10.1016/j.buildenv.2005.10.035>.  
502 [12] Khattab SA, Al-Mukhtar M, Fleureau J-M. Long-Term Stability Characteristics of  
503 a Lime-Treated Plastic Soil. *J Mater Civ Eng* 2007;19:358–66.  
504 [https://doi.org/10.1061/\(ASCE\)0899-1561\(2007\)19:4\(358\)](https://doi.org/10.1061/(ASCE)0899-1561(2007)19:4(358)).  
505 [13] Chittoori BS, Puppala AJ, Saride S, Nazarian S, Hoyos LR. Durability studies of  
506 lime stabilized clayey soils. *Proceedings of the 17th International Conference on*  
507 *Soil Mechanics and Geotechnical Engineering*, 2008, p. 5.  
508 [14] Alavéz-Ramírez R, Montes-García P, Martínez-Reyes J, Altamirano-Juárez DC,  
509 Gochi-Ponce Y. The use of sugarcane bagasse ash and lime to improve the

- 510 durability and mechanical properties of compacted soil blocks. *Construction and*  
511 *Building Materials* 2012;34:296–305.  
512 <https://doi.org/10.1016/j.conbuildmat.2012.02.072>.
- 513 [15] Neramitkornburi A, Horpibulsuk S, Shen SL, Chinkulkijniwat A, Arulrajah A,  
514 Disfani MM. Durability against wetting–drying cycles of sustainable Lightweight  
515 Cellular Cemented construction material comprising clay and fly ash wastes.  
516 *Construction and Building Materials* 2015;77:41–9.  
517 <https://doi.org/10.1016/j.conbuildmat.2014.12.025>.
- 518 [16] Dempsey BJ, Thompson MR. Durability Properties of Lime-Soil Mixtures.  
519 *Highway Research Records* 235 1968:15.
- 520 [17] Bin-Shafique S, Rahman K, Yaykiran M, Azfar I. The long-term performance of  
521 two fly ash stabilized fine-grained soil subbases. *Resources, Conservation and*  
522 *Recycling* 2010;54:666–72. <https://doi.org/10.1016/j.resconrec.2009.11.007>.
- 523 [18] Consoli NC, Marques SFV, Floss MF, Festugato L. Broad-Spectrum Empirical  
524 Correlation Determining Tensile and Compressive Strength of Cement-Bonded  
525 Clean Granular Soils. *J Mater Civ Eng* 2017;29:1–7.  
526 [https://doi.org/10.1061/\(ASCE\)MT.1943-5533.0001858](https://doi.org/10.1061/(ASCE)MT.1943-5533.0001858).
- 527 [19] Roshan K, Choobbasti AJ, Kutanaei SS. Evaluation of the impact of fiber  
528 reinforcement on the durability of lignosulfonate stabilized clayey sand under wet-  
529 dry condition. *Transportation Geotechnics* 2020;23:100359.  
530 <https://doi.org/10.1016/j.trgeo.2020.100359>.
- 531 [20] Tiwari N, Satyam N, Puppala AJ. Strength and durability assessment of expansive  
532 soil stabilized with recycled ash and natural fibers. *Transportation Geotechnics*  
533 2021;29:100556. <https://doi.org/10.1016/j.trgeo.2021.100556>.
- 534 [21] Buritatum A, Horpibulsuk S, Udomchai A, Suddepong A, Takaikaew T,  
535 Vichitcholchai N, et al. Durability improvement of cement stabilized pavement  
536 base using natural rubber latex. *Transportation Geotechnics* 2021;28:100518.  
537 <https://doi.org/10.1016/j.trgeo.2021.100518>.
- 538 [22] Hoy M, Rachan R, Horpibulsuk S, Arulrajah A, Mirzababaei M. Effect of wetting–  
539 drying cycles on compressive strength and microstructure of recycled asphalt  
540 pavement – Fly ash geopolymer. *Construction and Building Materials*  
541 2017;144:624–34. <https://doi.org/10.1016/j.conbuildmat.2017.03.243>.
- 542 [23] Cuisinier O, Masroufi F. Impact of wetting/drying cycles on the hydromechanical  
543 behaviour of a treated soil. *E3S Web Conf* 2020;195:1–6.  
544 <https://doi.org/10.1051/e3sconf/202019506008>.
- 545 [24] Stoltz G, Cuisinier O, Masroufi F. Weathering of a lime-treated clayey soil by  
546 drying and wetting cycles. *Engineering Geology* 2014;181:281–9.  
547 <https://doi.org/10.1016/j.enggeo.2014.08.013>.
- 548 [25] Consoli NC, Quiñónez Samaniego RA, González LE, Bittar EJ, Cuisinier O.  
549 Impact of Severe Climate Conditions on Loss of Mass, Strength, and Stiffness of  
550 Compacted Fine-Grained Soils–Portland Cement Blends. *J Mater Civ Eng*  
551 2018;30:04018174. [https://doi.org/10.1061/\(ASCE\)MT.1943-5533.0002392](https://doi.org/10.1061/(ASCE)MT.1943-5533.0002392).
- 552 [26] Pedarla A. Durability studies on stabilization effectiveness of soils containing  
553 different fractions of montmorillonite. University of Texas, 2009.
- 554 [27] Aldaood A, Bouasker M, Al-Mukhtar M. Impact of wetting–drying cycles on the  
555 microstructure and mechanical properties of lime-stabilized gypseous soils.  
556 *Engineering Geology* 2014;174:11–21.  
557 <https://doi.org/10.1016/j.enggeo.2014.03.002>.
- 558 [28] ASTM. D559/D559M – 15: Standard Test Methods for Wetting and Drying  
559 Compacted Soil-Cement Mixtures 2015.

- 560 [29] Cuisinier O, Masrouri F, Mehenni A. Alteration of the Hydromechanical  
561 Performances of a Stabilized Compacted Soil Exposed to Successive Wetting–  
562 Drying Cycles. *J Mater Civ Eng* 2020;32:04020349.  
563 [https://doi.org/10.1061/\(ASCE\)MT.1943-5533.0003270](https://doi.org/10.1061/(ASCE)MT.1943-5533.0003270).
- 564 [30] Menaceur H, Cuisinier O, Masrouri F, Eslami H. Impact of monotonic and cyclic  
565 suction variations on the thermal properties of a stabilized compacted silty soil.  
566 *Transportation Geotechnics* 2021;28:100515.  
567 <https://doi.org/10.1016/j.trgeo.2021.100515>.
- 568 [31] Packard RG, Chapman GA. Developments in Durability Testing of Soil-Cement  
569 Mixtures. *Highway Research Record* 1963;36:97–123.
- 570 [32] Hoyos LR, Laikram A, Puppala A. Assessment of seasonal effects on engineering  
571 behavior of chemically treated sulfate rich expansive clay., 2005, p. 483–504.
- 572 [33] Zhu W, Zhang CL, Chiu ACF. Soil–Water Transfer Mechanism for Solidified  
573 Dredged Materials. *J Geotech Geoenviron Eng* 2007;133:588–98.  
574 [https://doi.org/10.1061/\(ASCE\)1090-0241\(2007\)133:5\(588\)](https://doi.org/10.1061/(ASCE)1090-0241(2007)133:5(588)).
- 575 [34] Chiu CF, Zhu W, Zhang CL. Yielding and shear behaviour of cement-treated  
576 dredged materials. *Engineering Geology* 2009;103:1–12.  
577 <https://doi.org/10.1016/j.enggeo.2008.07.007>.
- 578 [35] Dadda A, Geindreau C, Emeriault F, Esnault Filet A, Garandet A. Influence of the  
579 microstructural properties of biocemented sand on its mechanical behavior. *Int J*  
580 *Numer Anal Methods Geomech* 2019;43:568–77.  
581 <https://doi.org/10.1002/nag.2878>.
- 582 [36] Leroueil S, Vaughan PR. The general and congruent effects of structure in natural  
583 soils and weak rocks. *Géotechnique* 1990;40:467–88.  
584 <https://doi.org/10.1680/geot.1990.40.3.467>.
- 585 [37] Burland JB, Dean ETR, Gudehus G, Muhunthan B, Collins IF. Discussion:  
586 Interlocking, and peak and design strengths. *Géotechnique* 2008;58:527–32.  
587 <https://doi.org/10.1680/geot.2008.58.6.527>.
- 588 [38] Robin V, Cuisinier O, Masrouri F, Javadi A. A chemo-mechanical coupling for lime  
589 treated soils. In: Soga K, Kumar K, Biscontin G, Kuo M, editors. *Geomechanics*  
590 *from Micro to Macro*, CRC Press; 2014, p. 1531–6.  
591 <https://doi.org/10.1201/b17395-278>.
- 592 [39] Rowe PW. The stress-dilatancy relation for static equilibrium of an assembly of  
593 particles in contact. *Proc R Soc Lond A* 1962;269:500–27.  
594 <https://doi.org/10.1098/rspa.1962.0193>.
- 595 [40] Cuccovillo T, Coop MR. On the mechanics of structured sands. *Géotechnique*  
596 1999;49:741–60. <https://doi.org/10.1680/geot.1999.49.6.741>.
- 597 [41] Wang L, Chu J, Wu S, Wang H. Stress–dilatancy behavior of cemented sand:  
598 comparison between bonding provided by cement and biocement. *Acta Geotech*  
599 2021. <https://doi.org/10.1007/s11440-021-01146-4>.
- 600 [42] AFNOR. NF EN 16907-2: Terrassement — Partie 2 : Classification des matériaux  
601 2018.
- 602 [43] ASTM. Standard Practice for Classification of Soils for Engineering Purposes  
603 (Unified Soil Classification System). ASTM International; 2020.  
604 <https://doi.org/10.1520/D2487-17E01>.
- 605 [44] AFNOR. NF EN 196-1 : Méthodes d'essais des ciments - Partie 1 : détermination  
606 des résistances 2016.
- 607 [45] AFNOR. NF EN 196-3 : Méthodes d'essai des ciments - Partie 3 : détermination  
608 du temps de prise et de la stabilité. 2017.

- 609 [46] AFNOR. NF EN 13286-53 : Mélanges traités et mélanges non traités aux liants  
610 hydrauliques. Partie 53 : Méthode de confection par compression axiale des  
611 éprouvettes de matériaux traités aux liants hydrauliques 2005.
- 612 [47] Mehenni A. Comportement hydromécanique et érosion des sols fins traités.  
613 Université de Lorraine, 2015.
- 614 [48] Roscoe KH, Schofield AN, Thurairajah A. Yielding of Clays in States Wetter than  
615 Critical. *Géotechnique* 1963;13:211–40.  
616 <https://doi.org/10.1680/geot.1963.13.3.211>.
- 617 [49] Malandraki V, Toll DG. The definition of yield for bonded materials. *Geotechnical  
618 and Geological Engineering* 1996;14:16.
- 619 [50] AFNOR. NF EN ISO 17892-9 : Reconnaissance et essais géotechniques - Essais  
620 de laboratoire sur les sols - Partie 9 : essais en compression à l'appareil triaxial  
621 consolidés sur sols saturés 2018.
- 622 [51] Wang YH, Leung SC. Characterization of Cemented Sand by Experimental and  
623 Numerical Investigations. *J Geotech Geoenviron Eng* 2008;134:992–1004.  
624 [https://doi.org/10.1061/\(ASCE\)1090-0241\(2008\)134:7\(992\)](https://doi.org/10.1061/(ASCE)1090-0241(2008)134:7(992)).
- 625 [52] Wu S, Li B, Chu J. Stress-Dilatancy Behavior of MICP-Treated Sand. *Int J  
626 Geomech* 2021;21:04020264. [https://doi.org/10.1061/\(ASCE\)GM.1943-  
627 5622.0001923](https://doi.org/10.1061/(ASCE)GM.1943-5622.0001923).
- 628 [53] Salih RO, Maulood AO. Influence of temperature and cycles of wetting and drying  
629 on modulus of rupture. *Soil and Tillage Research* 1988;11:73–80.  
630 [https://doi.org/10.1016/0167-1987\(88\)90032-3](https://doi.org/10.1016/0167-1987(88)90032-3).
- 631 [54] Bachmann J, Söffker S, Sepehrnia N, Goebel M, Woche SK. The effect of  
632 temperature and wetting–drying cycles on soil wettability: Dynamic molecular  
633 restructuring processes at the solid–water–air interface. *Eur J Soil Sci*  
634 2021;72:2180–98. <https://doi.org/10.1111/ejss.13102>.
- 635 [55] Lemaire K, Deneele D, Bonnet S, Legret M. Effects of lime and cement treatment  
636 on the physicochemical, microstructural and mechanical characteristics of a  
637 plastic silt. *Engineering Geology* 2013;166:255–61.  
638 <https://doi.org/10.1016/j.enggeo.2013.09.012>.
- 639

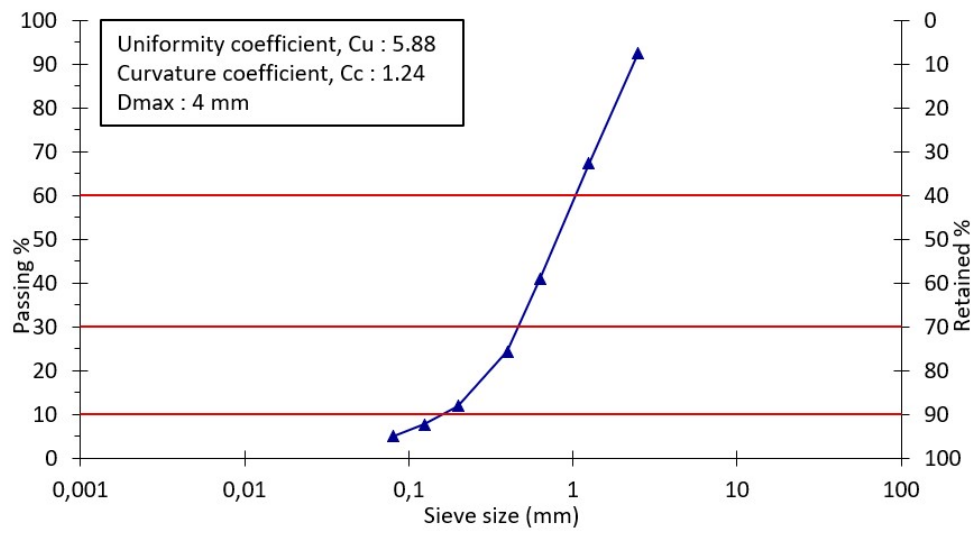


Fig. 1: Grain-size distribution of the studied sand.

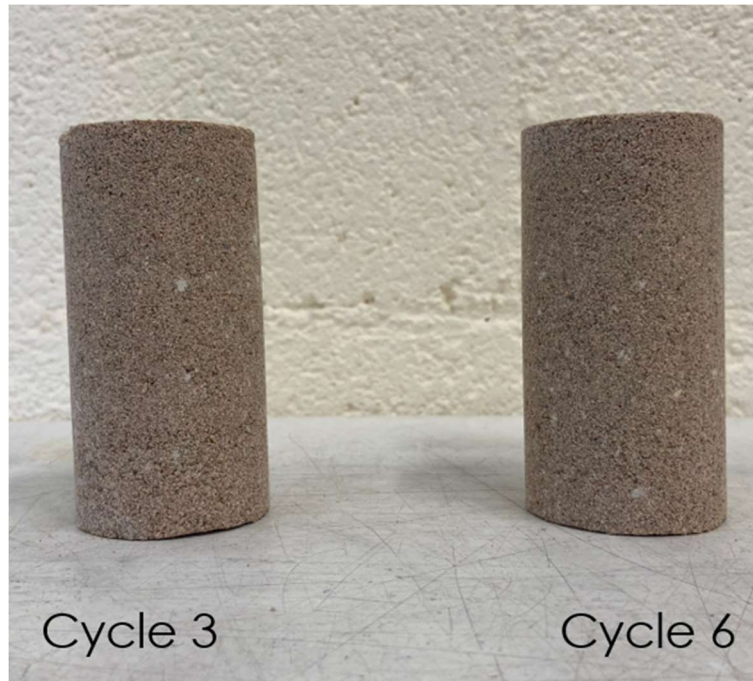


Fig. 2: Samples treated with 4% of cement after 3 type I-cycles and after 6 type-I cycles.

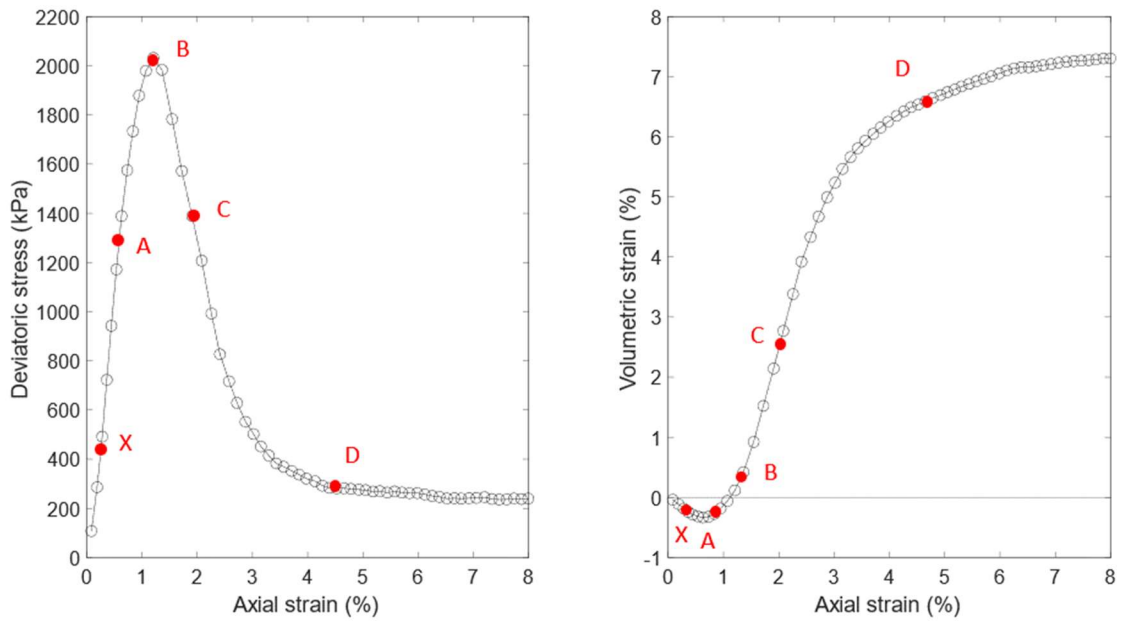


Fig. 3: Illustration of the points A, B, C, D and X on triaxial results of a 6%-cement-stabilized sand (for a confining pressure of 50 kPa).

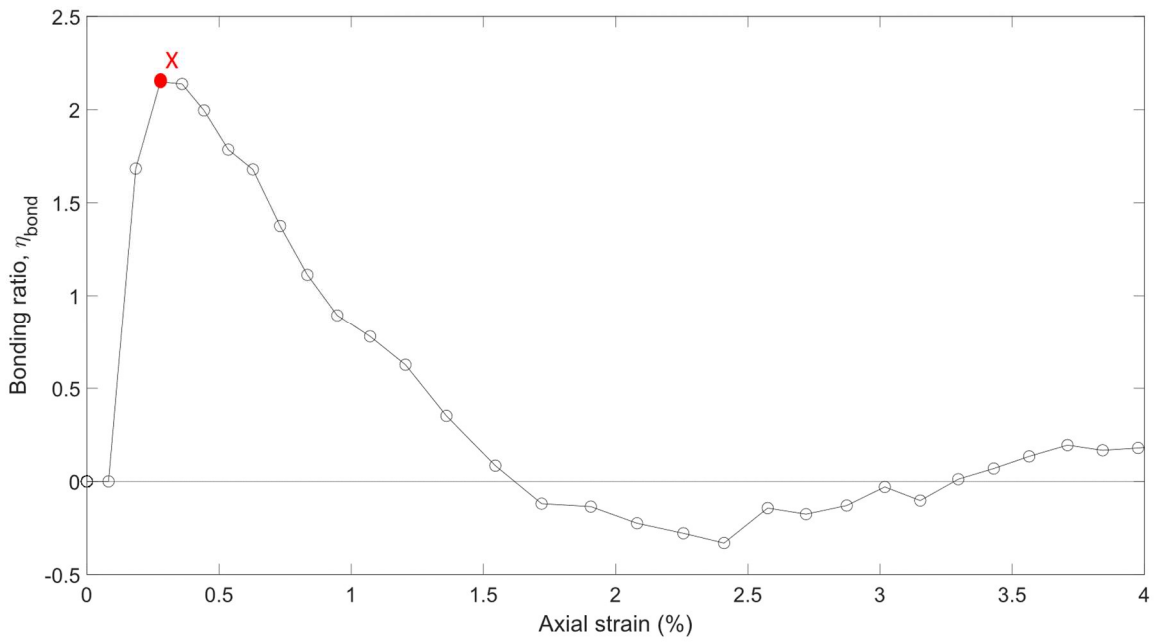


Fig. 4: Evolution of the bonding ratio during triaxial shearing on a 6%-cement-stabilized sand under a confining pressure of 50 kPa.

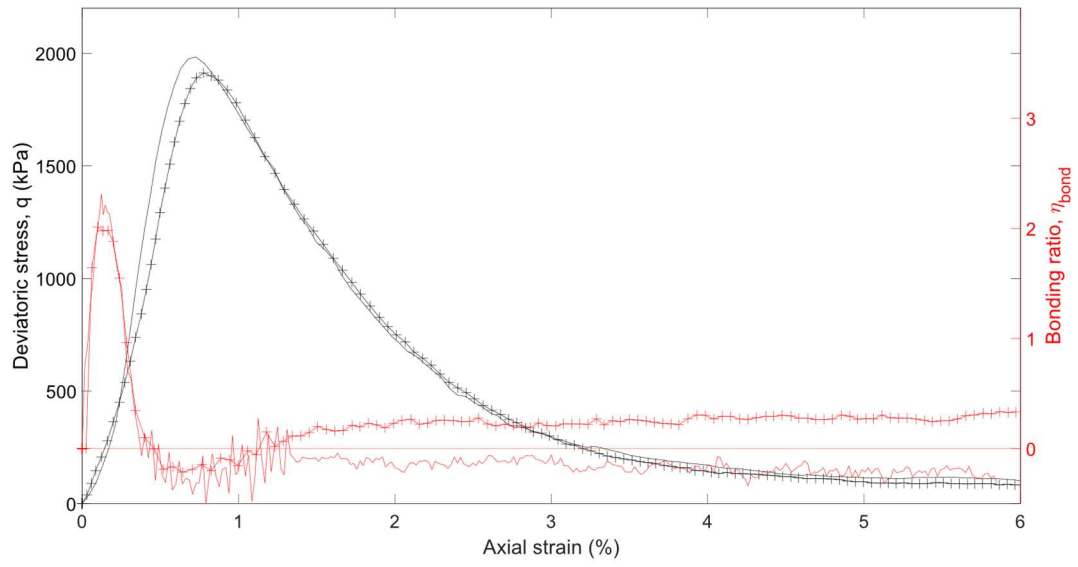


Fig. 5: Specimens treated with 6% cement at different curing time (for a confining pressure of 50 kPa). Stress-strain curves (black) and bonding ratio (red).

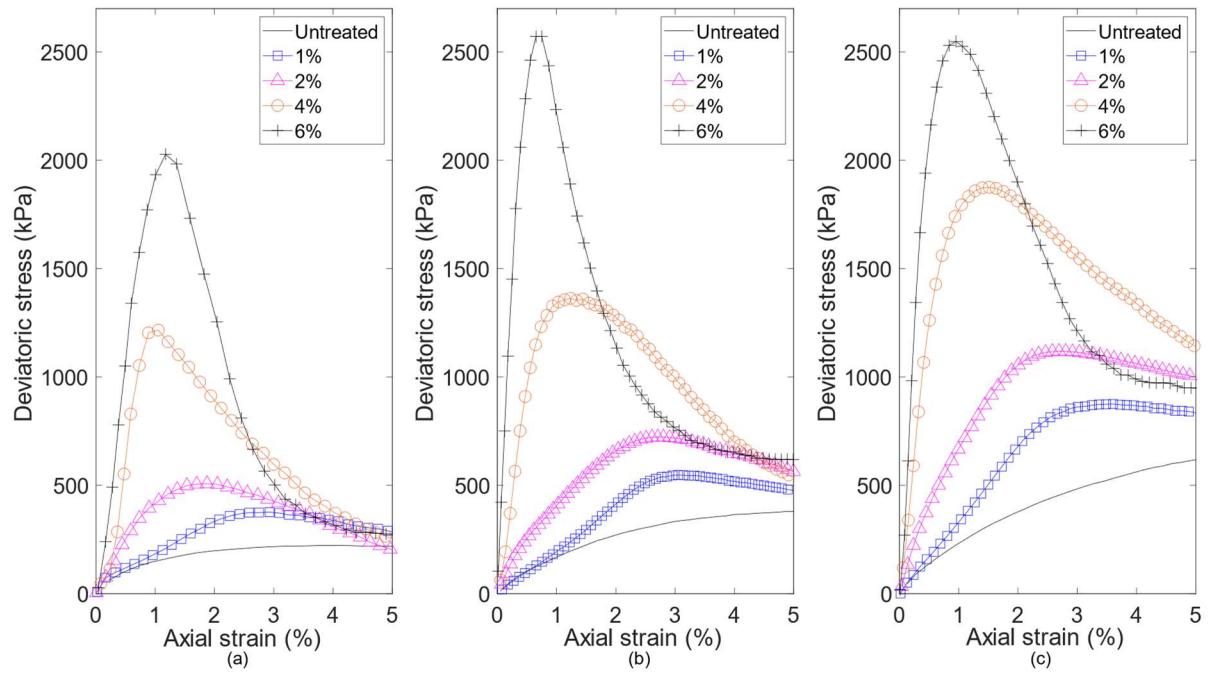


Fig. 6: Stress-strain curves for untreated and cement-treated sand under 50 (a), 100 (b) and 200 kPa (c) of confining pressure.

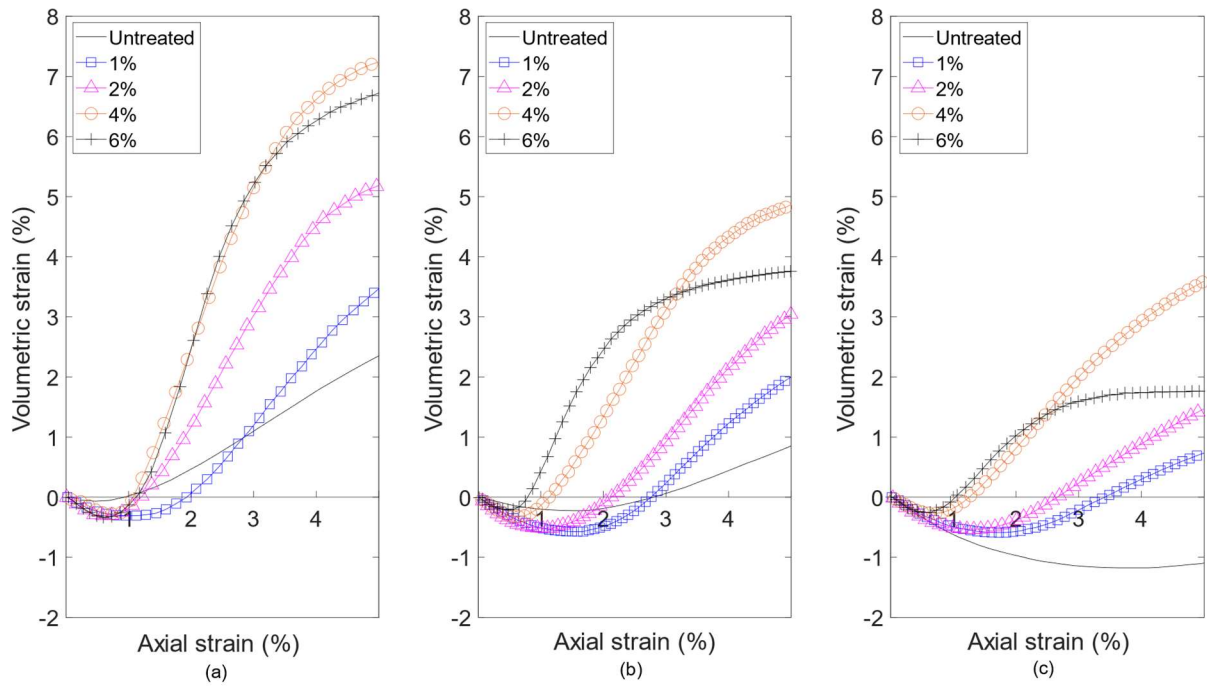


Fig. 7: Volumetric strain behavior for untreated and cement-treated sand under 50 (a), 100 (b) and 200 kPa (c) of confining pressure.

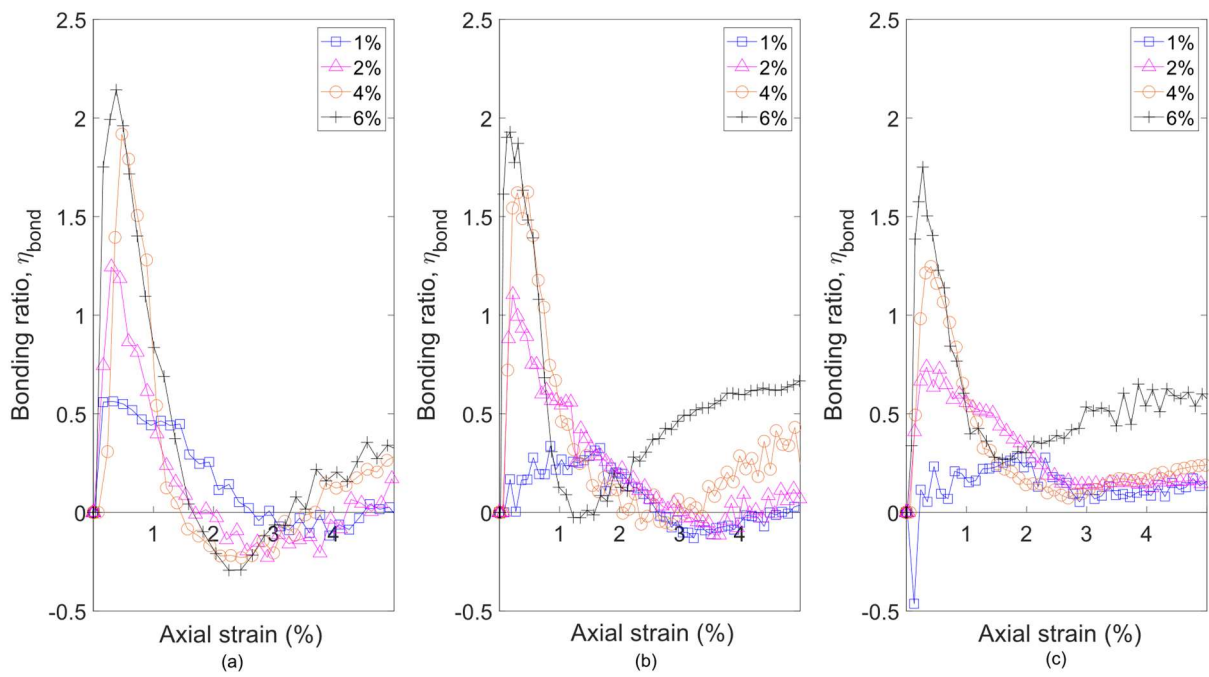
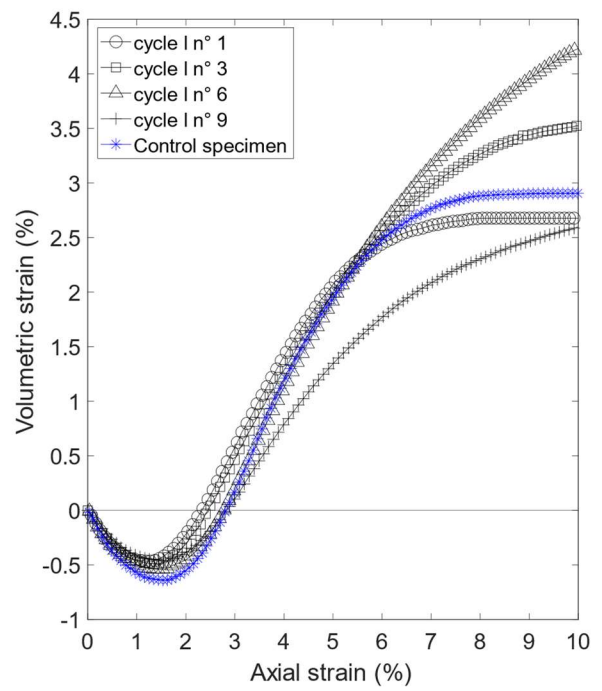
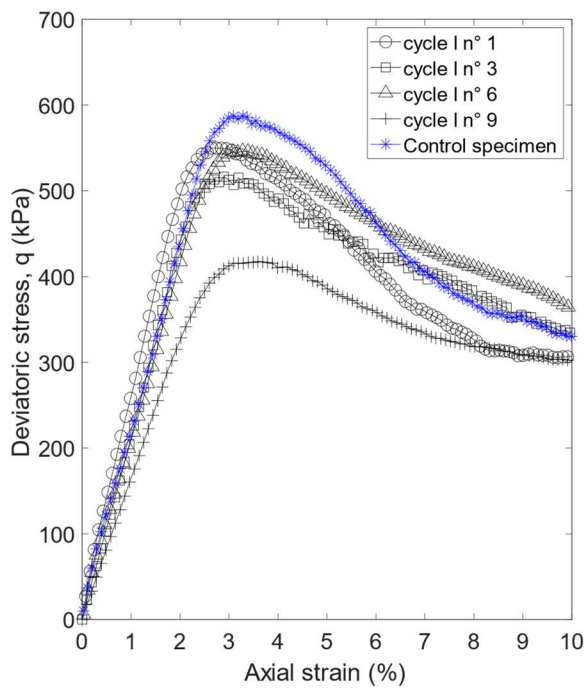
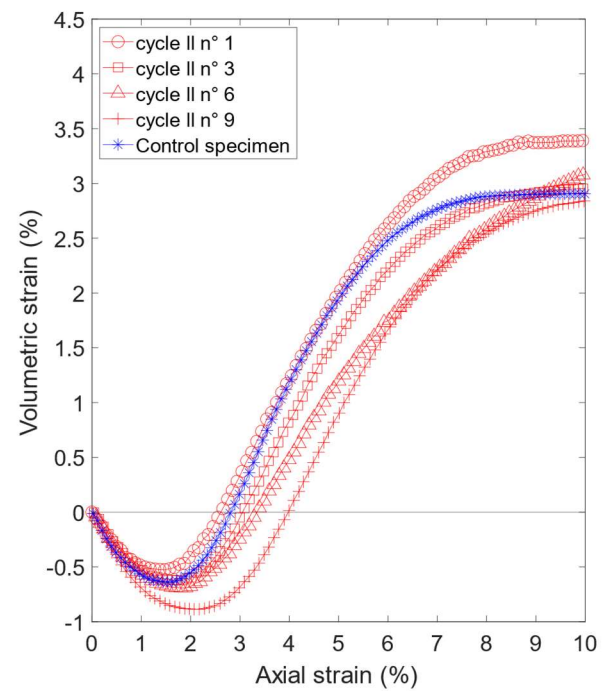
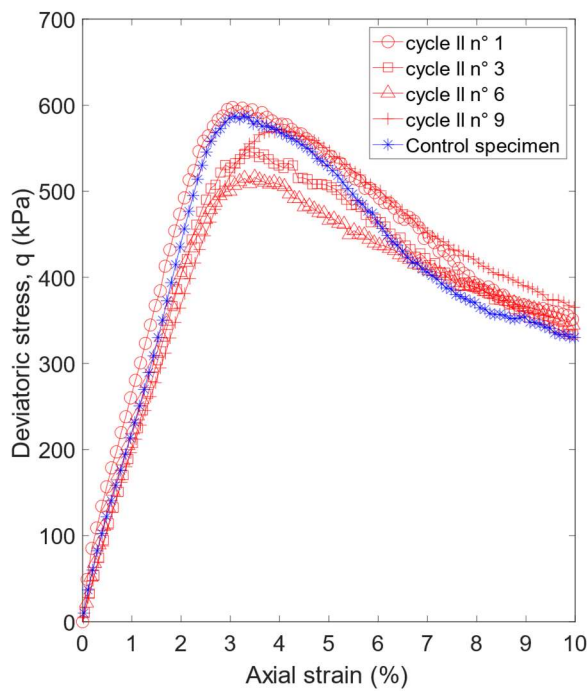


Fig. 8: Bonding ratio for untreated and cement-treated sand under 50 (a), 100 (b) and 200 kPa (c) of confining pressure.

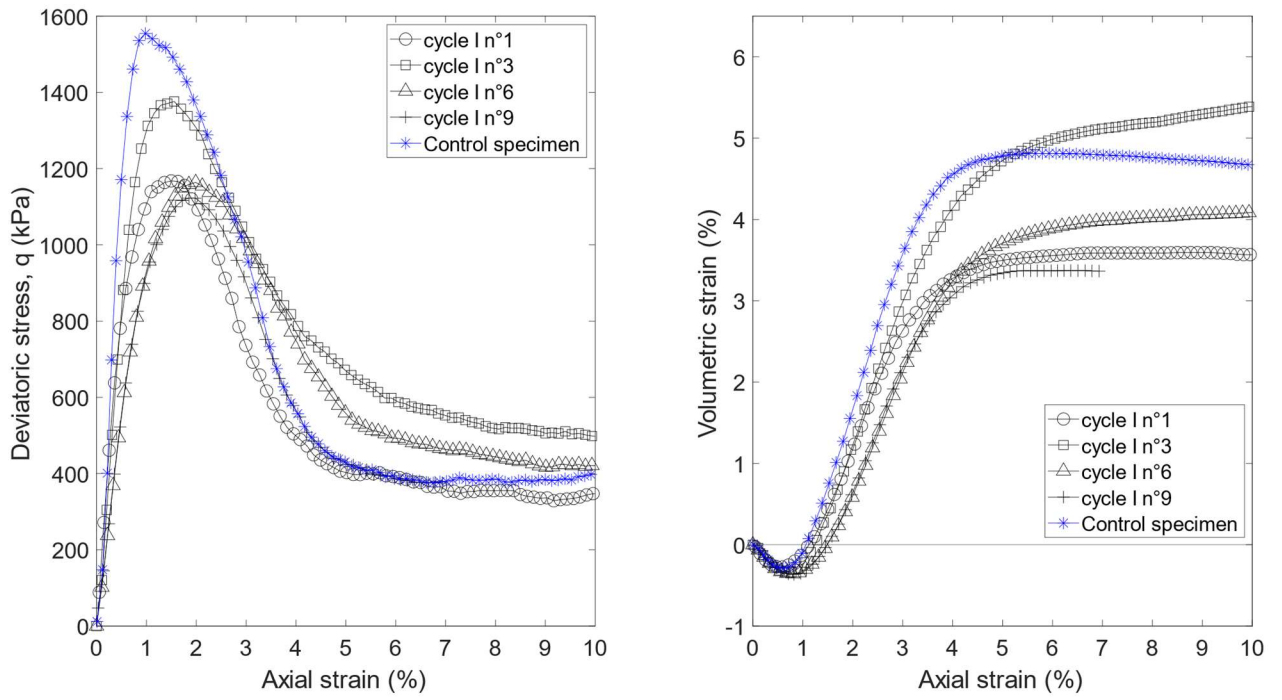


(a)

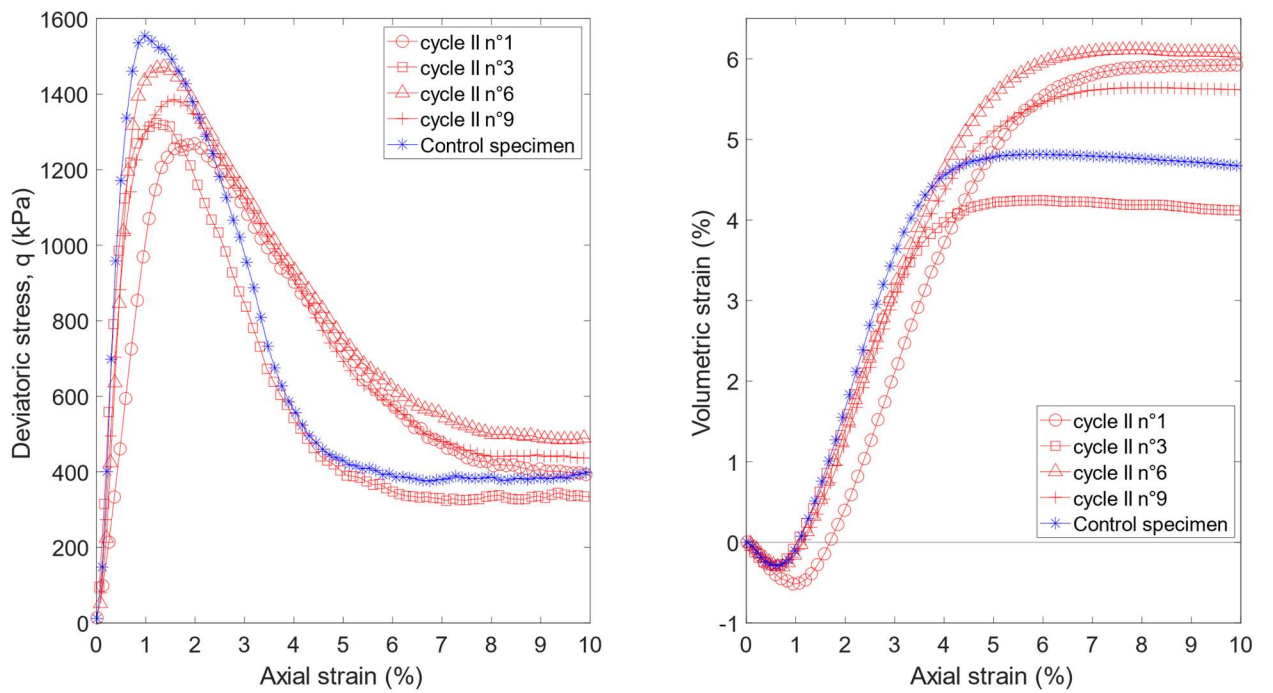


(b)

Fig. 9a and b: Influence of the type and the numbers of wetting-drying cycles on the stress-strain and volumetric strain curves for sand treated with 1% of cement under 100 kPa of confining pressure.

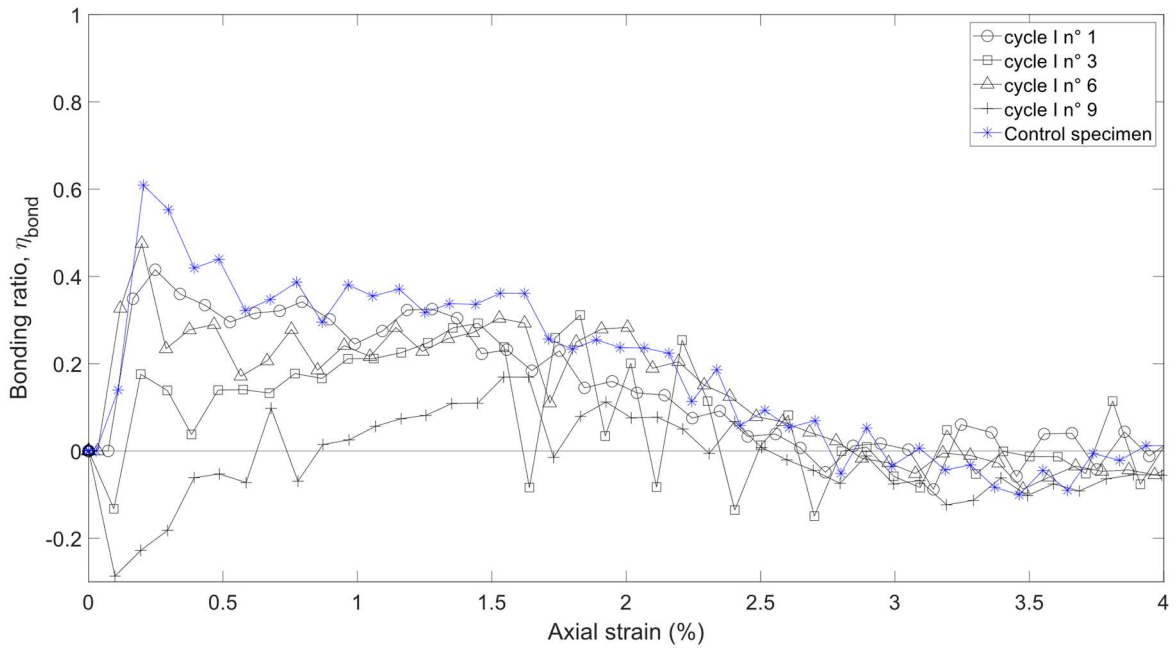


(a)

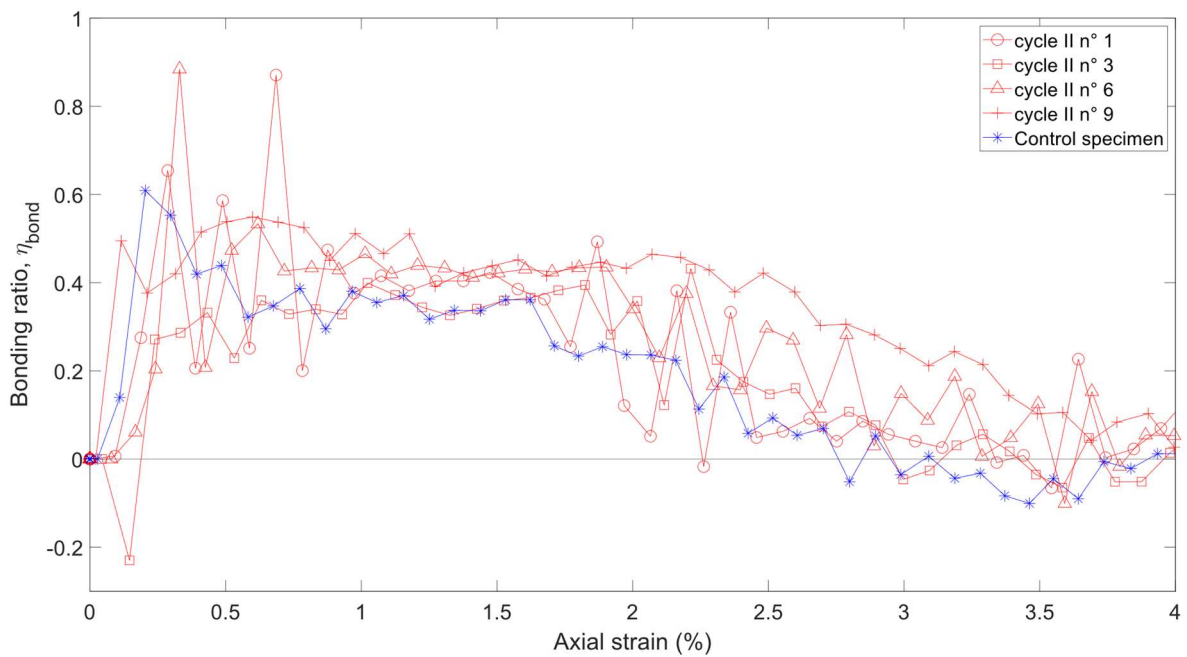


(b)

Fig. 10a and b: Influence of the type and the numbers of wetting-drying cycles on the stress-strain and volumetric strain curves for sand treated with 4% of cement under 100 kPa of confining pressure.

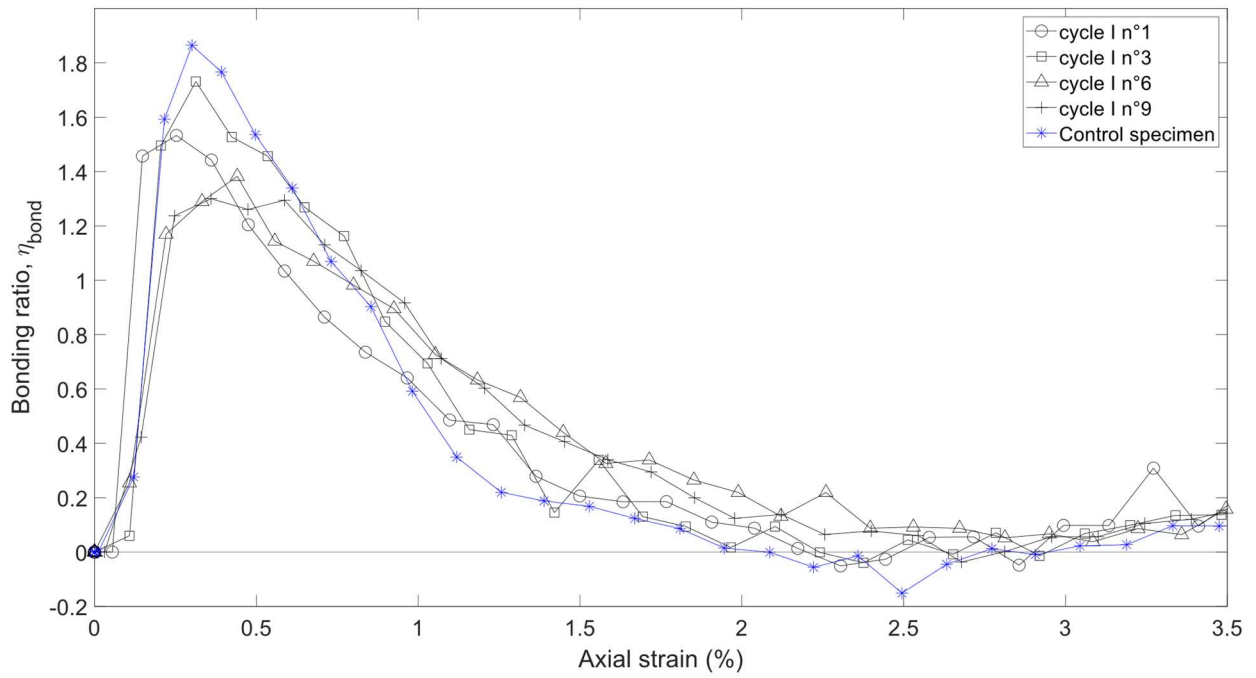


(a)

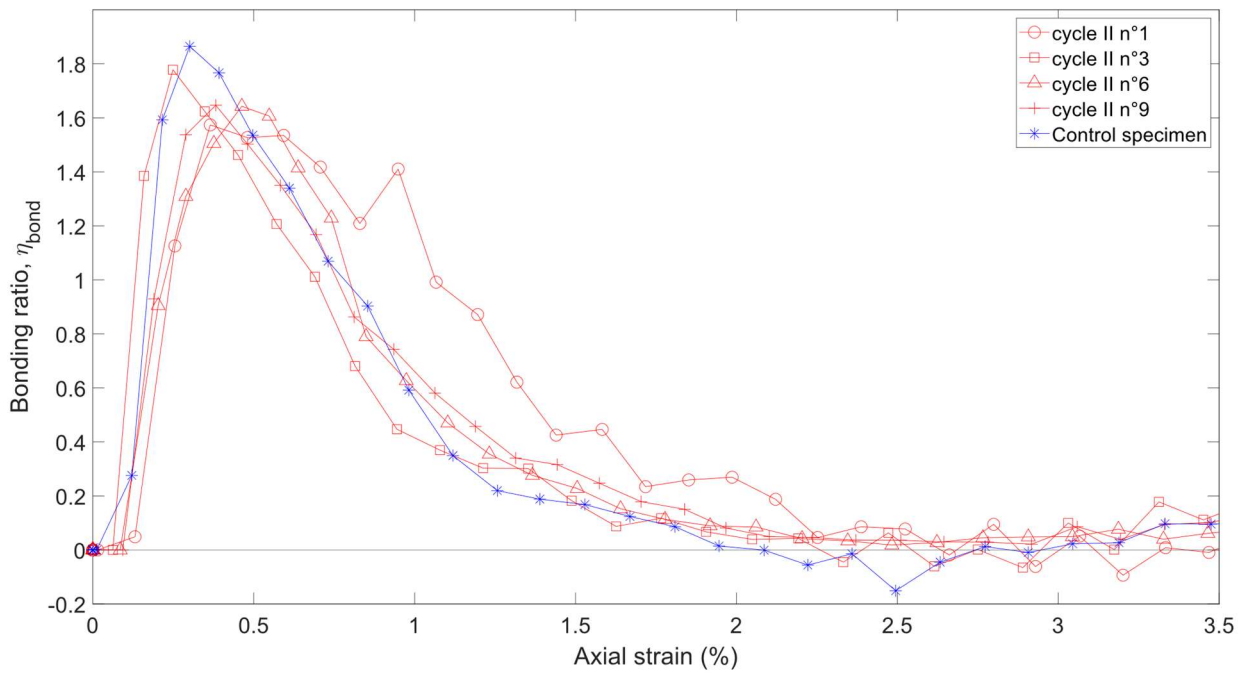


(b)

Fig. 11a and b: Influence of the type and the numbers of wetting-drying cycles on the bonding ratio for sand treated with 1% of cement under 100 kPa of confining pressure.

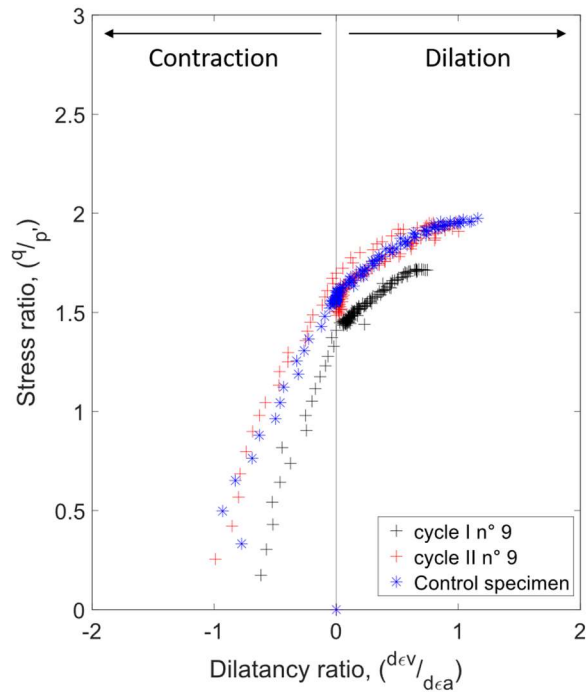


(a)

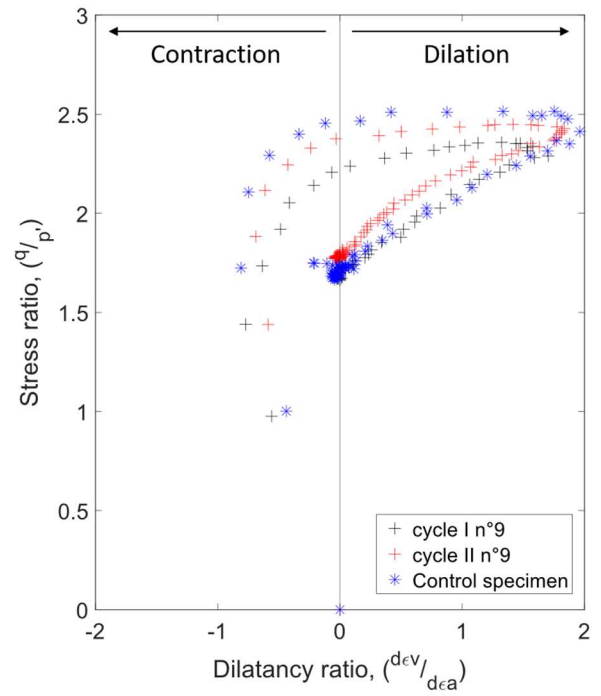


(b)

Fig. 12a and b: Influence of the type and the numbers of wetting-drying cycles on the bonding ratio curves for sand treated with 4% of cement under 100 kPa of confining pressure.



(a)



(b)

Fig. 13: Stress ratio  $(q/p)$  as a function of the dilatancy ratio  $(d)$  a. 1% of cement b. 4% of cement.

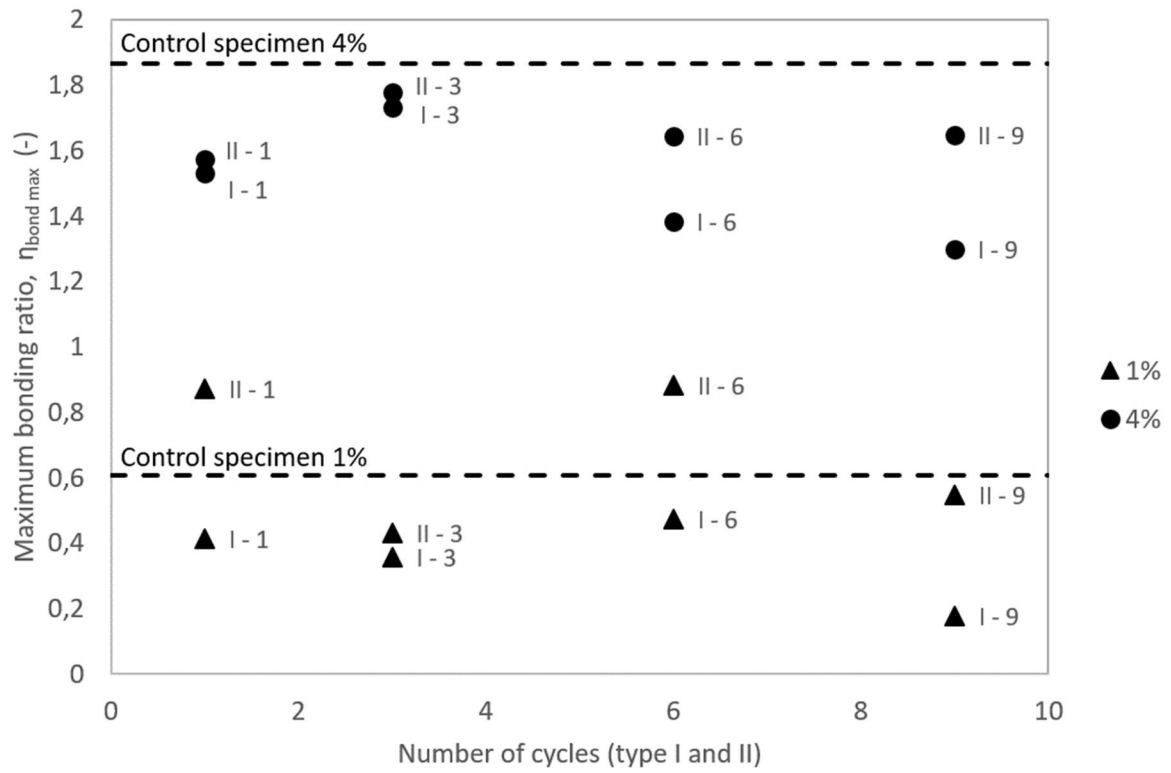


Fig. 14: Bonding ratio as a function of the type of cycles and the number of cycles for 1% and 4% cement content.

Table 1 : Geotechnical properties of the studied sand

| Characteristics    | Value |
|--------------------|-------|
| Maximum void ratio | 0.69  |
| Minimum void ratio | 0.52  |
| Specific gravity   | 2.63  |

Table 2: Cohesion and friction angle as a function of the cement content

| Cement content | Cohesion (kPa) | Friction angle (°) |
|----------------|----------------|--------------------|
| 0              | 0              | 37                 |
| 1%             | 48             | 39                 |
| 2%             | 64             | 42                 |
| 4%             | 198            | 44                 |
| 6%             | 388            | 44                 |

Table 3: Points A, B, C, D and X as functions of the cement content and the confining pressure

| Cement content (%) | Confining pressure (kPa) | A - $q$ (kPa) | B - $q_{max}$ (kPa) | C - dilatancy ratio ( $d$ ) | D - $q$ (kPa) | X - $\eta_{bond\ max}$ |
|--------------------|--------------------------|---------------|---------------------|-----------------------------|---------------|------------------------|
|                    | 50                       | -             | -                   | -                           | -             | -                      |
| 0                  | 100                      | -             | -                   | -                           | -             | -                      |
|                    | 200                      | -             | -                   | -                           | -             | -                      |
|                    | 50                       | 326           | 377                 | 1.39                        | 268           | 0.5635                 |
| 1                  | 100                      | 441           | 548                 | 1.09                        | 385           | 0.3366                 |
|                    | 200                      | 704           | 875                 | 0.56                        | 580           | 0.2931                 |
|                    | 50                       | 348           | 508                 | 2.01                        | 144           | 1.2447                 |
| 2                  | 100                      | 632           | 723                 | 1.36                        | 400           | 1.1049                 |
|                    | 200                      | 871           | 1119                | 0.70                        | 715           | 0.7367                 |
|                    | 50                       | 830           | 1217                | 2.99                        | 182           | 2.4606                 |
| 4                  | 100                      | 1043          | 1363                | 2.01                        | 460           | 1.6241                 |
|                    | 200                      | 1261          | 1876                | 1.24                        | 834           | 1.2471                 |
|                    | 50                       | 1340          | 2028                | 3.58                        | 277           | 2.1426                 |
| 6                  | 100                      | 1777          | 2571                | 2.50                        | 655           | 1.9287                 |
|                    | 200                      | 1668          | 2548                | 1.20                        | 911           | 1.751                  |

Table 4: Points A, B, C, D and X for samples treated with 1% of cement as functions of the type and number of cycles (considering a confining pressure of 100 kPa)

| Cement content (%) and Cycle type | Number of cycles | A - $q$ (kPa) | B - $q_{max}$ (kPa) | C - dilatancy ratio ( $d$ ) | D - $q$ (kPa) | X - $\eta_{bond\ max}$ |
|-----------------------------------|------------------|---------------|---------------------|-----------------------------|---------------|------------------------|
| 1 - I                             | 1                | 447           | 550                 | 0.998                       | 319           | 0.4615                 |
| 1 - I                             | 3                | 412           | 518                 | 1.071                       | 357           | 0.323                  |
| 1 - I                             | 6                | 457           | 547                 | 1.007                       | 397           | 0.3647                 |
| 1 - I                             | 9                | 288           | 417                 | 0.7459                      | 319           | 0.1662                 |
| 1 - II                            | 1                | 513           | 598                 | 1.083                       | 370           | 0.6771                 |
| 1 - II                            | 3                | 444           | 547                 | 1.034                       | 363           | 0.4027                 |
| 1-control II                      | 3                | 456           | 587                 | 1.159                       | 357           | 0.5886                 |
| 1 - II                            | 6                | 434           | 516                 | 0.9398                      | 370           | 0.5664                 |
| 1 - II                            | 9                | 494           | 571                 | 1.002                       | 397           | 0.8478                 |

Table 5: Points A, B, C, D and X for samples treated with 4% of cement as functions of the type and number of cycles (considering a confining pressure of 100 kPa)

| Cement content (%) and Cycle type | Number of cycles | A - q (kPa) | B - q <sub>max</sub> (kPa) | C - dilatancy ratio (d) | D - q (kPa) | X - $\eta_{\text{bond max}}$ |
|-----------------------------------|------------------|-------------|----------------------------|-------------------------|-------------|------------------------------|
| 4 - I                             | 1                | 781         | 1173                       | 1.705                   | 410         | 1.5608                       |
| 4 - I                             | 3                | 1049        | 1371                       | 1.903                   | 517         | 1.7142                       |
| 4 - I                             | 6                | 719         | 1165                       | 1.572                   | 440         | 1.3823                       |
| 4 - I                             | 9                | 826         | 1123                       | 1.703                   | 410         | 1.3191                       |
| 4 - II                            | 1                | 1070        | 1269                       | 1.909                   | 428         | 1.723                        |
| 4 - II                            | 3                | 986         | 1323                       | 1.971                   | 335         | 1.9644                       |
| 4 - II                            | 6                | 1036        | 1470                       | 1.863                   | 499         | 1.6392                       |
| 4 - II                            | 9                | 1031        | 1385                       | 1.833                   | 440         | 1.7609                       |
| 4-control II                      | 9                | 959         | 1554                       | 2.243                   | 410         | 1.9157                       |

## Highlights

- The degradation of performance after wetting and drying cycles is quantified through a stress-dilatancy approach.
- The extent of the degradation is function of the intensity of the wetting and drying cycles.
- The degradation process varies as a function of the binder dosage.
- The results highlight the role of the imposed wetting/drying cycles technique for a better assessment of the long-term performance of treated soils.